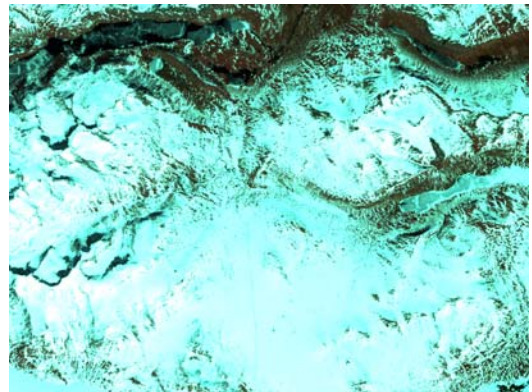


Snow grain size from satellite images

A review



Note no

SAMBA/31/09

Authors

Hans Koren

Date

December 2009

Norsk Regnesentral

Norsk Regnesentral (Norwegian Computing Center, NR) is a private, independent, non-profit foundation established in 1952. NR carries out contract research and development projects in the areas of information and communication technology and applied statistical modelling. The clients are a broad range of industrial, commercial and public service organizations in the national as well as the international market. Our scientific and technical capabilities are further developed in co-operation with The Research Council of Norway and key customers. The results of our projects may take the form of reports, software, prototypes, and short courses. A proof of the confidence and appreciation our clients have for us is given by the fact that most of our new contracts are signed with previous customers.

Title	Snow grain size from satellite images
Authors	Hans Koren
Date	December
Year	2009
Publication number	SAMBA/31/09

Abstract

This note is a review of works on retrieval of snow grain size from satellite images. A theoretical background is given and a number of models and algorithms are described. Most of the works are based on Landsat images with 30 m resolution and 7 optical channels, but the hyperspectral airborne AVIRIS sensor with 20 m resolution, and SAR has also been used.

An algorithm derived from Landsat images, has been modified to be used on MODIS images with 500 m resolution at NR. This is briefly described.

Keywords	Snow, grain size, satellite images
Target group	Snow hydrology, climatology, meteorology
Availability	Open
Project number	54
Research field	Earth observation
Number of pages	27
© Copyright	Norsk Regnesentral

Contents

1	Background	7
1.1	Properties of snow grains.....	7
1.2	Development of snow grains through the year.	8
1.3	Scattering model	9
1.4	Penetration depth.....	9
2	Methods	10
2.1	Landsat TM	10
2.1.1	Ratio between TM channels.....	16
2.2	AVIRIS	18
2.3	SAR	23
3	Conclusions	24
4	References	25

1 Background

1.1 Properties of snow grains

The monitoring of snow from satellites uses reflected sunlight, emission and backscatter of microwaves to determine snow parameters. The signals measured at the satellite will vary with the snow grain size. If you know the grain size, this will help in retrieval of other snow characteristics like snow cover extent, snow depth and snow wetness. When calculating the snow cover area, the reflectance measured in one pixel is compared with the reflectance measured in a control pixel with 100% snow cover. If the reflectance has a lower value, this could mean that the area within the pixel has some regions without snow. A decrease of the reflectance in the near infrared could also be caused by a change in the grain size, even if the area is totally covered by snow. Therefore, to get accurate values of other snow parameters, it is important to have methods to calculate the grain size directly.

Snow is a collection of ice grains and air, and, when at 0°C, it also has a significant fraction of liquid water. Snow also often contains absorbing impurities such as soot, dust, and pollen. The optical properties thus depend on the bulk optical properties and geometry of the ice grains, the liquid water inclusions, and the solid and soluble impurities. In the visible and near-infrared wavelengths, the bulk optical properties of ice and water are very similar, so the reflectance and transmittance of the snowpack in this region of the electromagnetic radiation spectrum depend on the wavelength variation of the refractive index of ice, the grain size distribution of the snow, the depth and density of the snowpack, and the size and amount of those impurities whose refractive indices are substantially different from those of ice and water.

The most important optical property of ice, which causes spectral variation in the reflectance of snow in visible and near-infrared wavelengths, is that the absorption coefficient varies by seven orders of magnitude at wavelengths from 0.4-2.5 micrometers.

Because ice is so transparent in the visible wavelengths, increasing the grain size does not appreciably affect the reflectance. The probability that a photon will be absorbed once it enters an ice grain is small, and that probability is not increasing very much if the ice grain is larger. Although the reflectance in the visible wavelengths is insensitive to grain size, it is affected by two variables, finite depth, and the presence of absorbing impurities. In the near-infrared, however, ice is moderately absorptive. Therefore, the reflectance is sensitive to grain size, and the sensitivity is greatest at 1.0-1.3 micrometers. Because the ice grains are strongly forward-scattering in the near-infrared, reflectance increases with illumination angle, especially for larger grains.

In Figure 1 the directional-hemispherical reflectance is shown for two values of the illumination angle for different grain sizes. We see that for the visible wavelengths (0.4 – 0.7 μm) reflectance is insensitive to grain size. In the near infrared, especially from 0.9 to 1.3 μm , reflectance is very sensitive to grain size. From 1.55 to 1.7 μm

reflectance is sensitive, but only for small sizes. We also see an increase in reflectance with illumination angle. This effect is greatest in the near infrared.

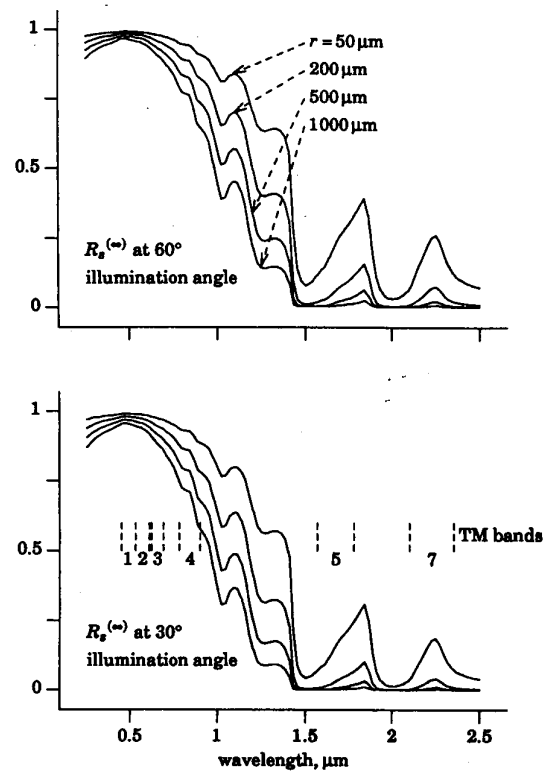


Figure 1 Directional-hemispherical reflectance R of deep snow at angles 60° and 30° , for wavelengths from 0.4 to $2.5 \mu\text{m}$. The curves represent grain radii of $50 \mu\text{m}$ (upper), $200 \mu\text{m}$, $500 \mu\text{m}$, and $1000 \mu\text{m}$ (lower). (Dozier, 1989).

The presence of liquid water in the snow does not by itself greatly affect the reflectance. Except for meltwater ponds in depressions, where melting snow overlies an impermeable substrate, liquid water content in snow rarely exceeds 5 or 6%. This small amount of water does not appreciably affect the bulk radiative-transfer properties, except possibly in those wavelength regions where the absorption coefficients of liquid water and ice are appreciably different. Instead, the changes in reflectance that occur in melting snow in large part result from the increased crystal sizes and from an effective size increase caused by the two-to-four grain clusters that form in wet unsaturated snow. These apparently behave optically as single grains, causing decreased reflectance in near-infrared wavelengths.

1.2 Development of snow grains through the year

New fallen snow has a high degree of dendricity. The size and irregularity of the snowflakes depend on temperature and wind. Fairly soon the grains start a metamorphism that will continue through the winter season. The particles with the highest surface-to-volume ratio will change most quickly. The dendrites will start to be reduced and eventually disappear. Initially the grain size will decrease, but when the

branches have disappeared, the average particle size will increase over time. The particles will be more rounded and single particles will join to create larger crystals.

Change in temperature will have a great influence on the metamorphism, especially if the temperature is near or at the melting point. The metamorphism will take place even if the temperature is kept constant, but especially if there is a temperature gradient through the snow pack. Throughout the season there will be changes in temperature and new snow will increase the pressure on the old snow. A general result is that the snow grains grow bigger and the grain size will increase with depth.

Due to the metamorphism the grain size will vary with the terrain. The grain size will vary with the temperature, and the temperature varies with elevation and solar incidence angle. Thus in a small area with large differences in elevation and slope angles, the grain size may have great variations. In steep slopes turning toward south, the metamorphism could run faster than in a slope towards north or a horizontal area at the same elevation. Thus a good knowledge of the topography could be a great help when trying to determine the grain size in an area. Meteorological data, like records of temperature and snowfall in a time period before the retrieval, will also be valuable.

1.3 Scattering model

The reflectance of snow is modelled as multiple scattering problem. Scattering properties of irregularly shaped grains are mimicked by Mie calculations for an “equivalent sphere”. Although snow grains are irregularly shaped, they are usually not oriented, so that the assumption that their scattering properties can be mimicked by some spherical radius r is reasonable, especially when we want to describe the general spectral properties.

Comparing snow grain sizes estimated from scattering models with grain sizes obtained from ground reference measurements, one has to be aware of the variation in size and regularity of the grains. The mean convex radius of the snow grains can be taken as an objective size indicator. But one should be aware that the measured grain size not always will be equivalent to the optical grain size found in the predictions by scattering models.

Near-field effects are assumed unimportant. The fact that the ice grains in a snowpack touch each other, apparently does not affect the snow’s reflectance, because the centre-to-centre spacing is still much larger than the wavelength. That is, snow reflectance is independent of density up to about 650 kg/m³. Reflectance measurements will show a significant inverse relationship between density and reflectance, but the physical model shows that the explanation for changes in reflectance lies in other properties of the snow cover, namely an increase in grain size and in the amount of contaminants near the surface.

1.4 Penetration depth

The penetration depth is determined primarily by the ratio of the grain size to the wavelength. The larger this ratio, the larger the penetration depth. Thus, the penetration

depth increases with increasing grain size for a fixed wavelength, and for a fixed grain size the penetration depth increases with decreasing wavelength.

For wavelengths in the near infrared the penetration depth vary from a few millimetres to many centimetres depending on the grain size and wavelength. Table 1 shows the penetration depth for four AVIRIS channels taken from Li et al. (2001).

Table 1 The penetration depth (cm) as a function of grain size for AVIRIS channels 54, 73, 93 and 145 (Li, 2001)

Grain size (μm)	Ch. 54 0.86 μm	Ch. 73 1.05 μm	Ch. 93 1.24 μm	Ch. 145 1.73 μm
50	3.3	1.2	0.57	0.19
100	4.8	1.8	0.83	0.27
200	6.9	2.6	1.2	0.39
500	11	4.1	1.9	0.65
1000	16	5.8	2.6	1.0
2000	22	8.1	3.7	1.8

As the grain size generally increases from the top layer and down, a shorter wavelength will get in contact with larger grains than a longer wavelength which will only be affected by the smaller grains in the top layer. The measured reflectance at 0.86 μm stems from the radiation backscattered by larger grains deeper within the snow than the radiation reflected at longer wavelengths. Thus, the grain size retrieved from the radiance measured at 0.86 μm will appear to be larger than that retrieved from the backscattered radiances at wavelengths 1.05 μm and 1.24 μm . At 1.73 μm , the wavelength is so long that the backscattered radiance is sensitive only to the smaller snow structure at the very top of the snow layer.

2 Methods

2.1 Landsat TM

Retrieval of grain size from Landsat Thematic Mapper images has been studied in a number of papers. Dozier (1989) has been studying the spectral signature of alpine snow cover. He also tried to find indicators for grain size from the measured reflectance in the various bands. In Figure 1 the reflectance as a function of wavelength is shown for various grain sizes and two solar incidence angles. The positions of the Thematic Mapper channels are marked on the figure. Here one can see that the reflectance is sensitive to the grain size especially in bands 4, 5 and 7, and particularly for small grain sizes for band 5 and 7. In Figure 2 modelled reflectance is presented as a function of grain size for TM4 and TM5 for two different solar incidence angles. If you compare Figure 1 and Figure 2 you will see that in Figure 1 the reflectance increases, and in Figure 2 it decreases with increasing illumination angle. This is because two different definitions of reflectance have been used. Figure 1 presents the directional hemispherical reflectance and in Figure 2 the modelled bidirectional reflectance from a nadir view is presented.

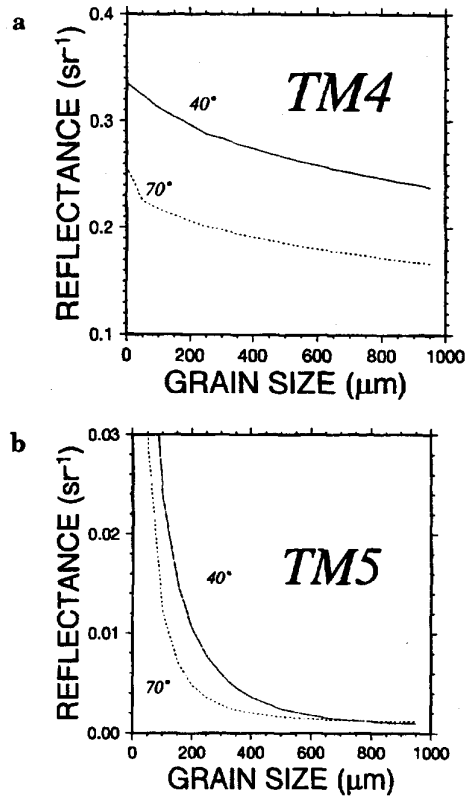


Figure 2 Modelled reflectance against grain size for two different wavelengths: (a) 0.85 μm (TM4) and (b) 1.65 μm (TM5). The surface is horizontal, the sun incidence angle is 40° (April) and 70° (December) and the view is nadir. (Fily, 1997). Be aware of the different reflectance scales for the two wavelengths. Compare Figure 5.

The largest sensitivity of snow reflectance to grain size occurs in the wavelengths from 1.0 to 1.3 μm , beyond the range of Thematic Mapper band 4 and below that of band 5.

Fily et al. (1997) tried to study in the detail the quantitative relation between Landsat reflectances and snow grain size. The snow reflectance was computed from TM data with and without atmospheric correction. Then the data were compared with theoretical results obtained from a bidirectional reflectance model. The estimates of grain size were compared with ground truth measurements at 11 different locations in the Alps. The experiments were done in April with sun incidence angle 40° and December 70°.

The bidirectional reflectance was computed with a model based on the solution of the radiative transfer equation through the discrete ordinate method, DISORT (Stamnes, 1988). The Mie theory is used to get the extinction coefficient and the phase function, which means that the snow grains are taken to be spherical and that interactions between grains are not taken into account. Because penetration depth is small in the infrared, a single layer of snow with a single grain size is assumed.

The dependency of reflectance on the grain size is shown in Figure 2 for TM4 and TM5. The results for TM7 are almost the same as those for TM5. From these curves, it is clear not only that the grain size can theoretically be obtained from the reflectance, but also that a precise value of the reflectance is needed to do so. For TM4 the curves are flat and very dependent on the incidence angle. A small error in the reflectance induces a large error in the grain size. For TM5 and TM7, there is a saturation effect for large grains, so it is difficult to precisely measure large grains. For smaller grain sizes there are large relative differences in the reflectance, even if the absolute differences are small.

Figure 3 gives the modelled bidirectional reflectances for channels TM4, TM5 and TM7 against the Landsat-derived bidirectional reflectances. The modelled reflectances are obtained by using the surface measured convex radius and the real slope. Each channel is represented by a single wavelength: 0.85 μm for TM4, 1.65 μm for TM5 and 2.2 μm for TM7. Each Landsat-derived reflectance is given with and without atmospheric corrections. The effect of atmospheric correction on the reflectance is important for TM4, but not for TM5 and TM7.

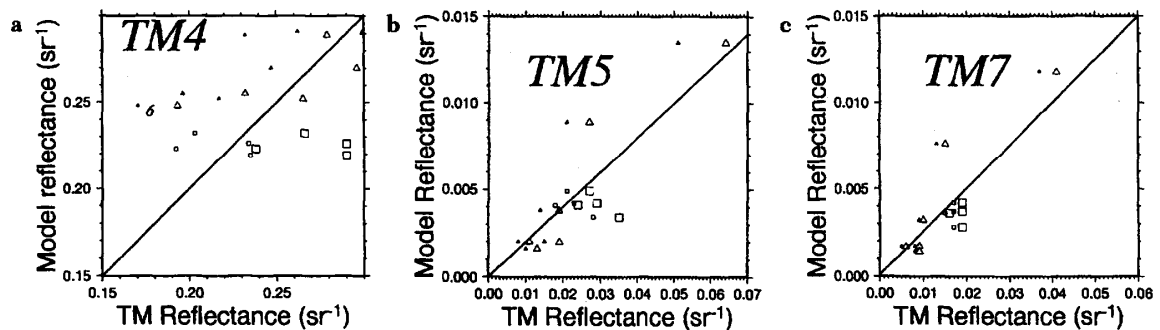


Figure 3 Modeled bidirectional reflectances against the measured reflectances derived from channels TM4 (a), TM5 (b), and TM7 (c). The model results are obtained by using ground data for the grain size and the real geometrical conditions. Triangles are for April, squares for December; small symbols are without atmospheric corrections, large symbols with atmospheric corrections. (Fily, 1997)

For TM4 most of the April data are close to the theory except for site 6. Although the snow cover was homogeneous, December corrected reflectances are too large and very scattered. It is probably mainly due to the topography. In the case of low sun elevation, the irradiance coming from facing slopes cannot be neglected. This effect is important for TM4 because the snow reflectance is high. In contrast, the reflectance of TM5 and TM7 is very low, so this effect becomes negligible.

It is not surprising to find different values of reflectance, mainly because the calibration coefficients are not very accurate and because the model does not exactly fit reality: The grains are not spherical, the mean convex radius may not be the optical effective radius, there is a distribution of grain sizes rather than a single size, and the model is not integrated over the channel spectral width.

It is surprising to find such a large difference for TM5 and TM7. The Landsat-derived reflectances are four or five times as large as the model results. The main reason for the discrepancy seems to be that the optical size of the grains is much smaller than the

measured mean convex radius. The penetration depth is so small at these wavelengths that the shape of the grains is very important. More measurements of the BRDF are clearly needed in this spectral range with simultaneous grain size measurements.

The variations of reflectances due to the grain size, the slope and the solar incidence angle are well reproduced for TM5 and TM7 (Figure 3). It should then be possible to try to deduce the grain size from the reflectance if an empirical correction is done.

For TM4, the Landsat-derived reflectances are not accurate enough to allow an inversion of the grain size from reflectance. For TM5 and TM7 empirical corrections are made, using linear relations. They are used to get a corrected reflectance (R_{corr}) from derived ground reflectances (R_{gr}) data:

$$\text{TM5 (all data): } R_{corr} = 0.4 * R_{gr}$$

$$\text{TM7 (all data): } R_{corr} = 0.5 * R_{gr}$$

Then the radius corresponding to the corrected reflectance and the geometric conditions of irradiance, measurement, and slope is searched by an iterative process (Stamnes, 1988). The radius is found when the difference between the modelled reflectance and the correct reflectance is less than 0.0001.

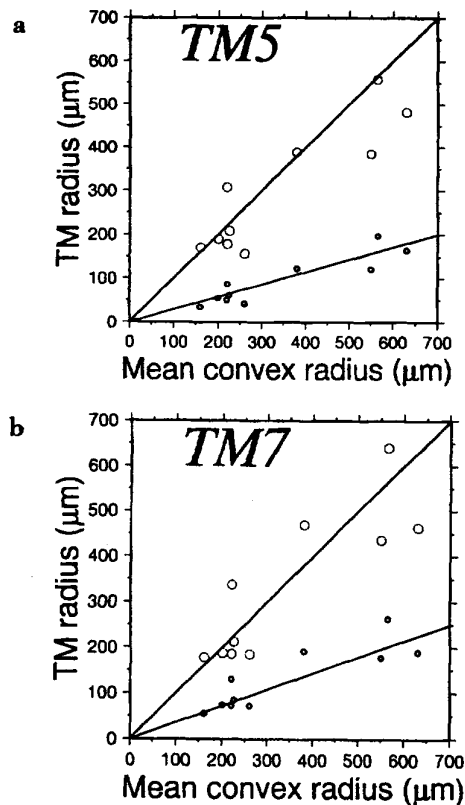


Figure 4 Comparison between the measured snow grain mean convex radius and the grain size derived from Landsat TM5 and TM7 data after an empirical correction of the reflectance (large circle) and without the correction (small circle) (Fily, 1997).

The results are given in Figure 4 together with the result of the same inversion procedure used on the uncorrected data.

The main problem is that the computed radii are different for TM5 and TM7 and those small sizes will not fit with the TM4 data. Therefore the optical grain size is different for different wavelengths. This effect has been confirmed by laboratory measurements made at Centre d'Etude de la Neige at Grenoble, but more studies are needed to better determine the size parameters that the model must take into account. The same effect is described in the works of Bourdelles and Fily (1993) and Li et al. (2001), see later in this chapter.

Bourdelles and Fily (1993) have studied a Landsat Thematic Mapper scene over Terre Adélie, Antarctica to estimate grain size. The Landsat data are coded on single byte numerical counts (NC) from 0 to 255. Radiances at satellite level are computed by:

$$L_{sat} = a_0 + a_1 NC$$

Where a_0 and a_1 are calibration coefficients. The apparent reflectance is:

$$\rho_{app} = \frac{L_{sat} \pi}{E_0 \cos \theta_i}$$

where E_0 is the solar irradiance in the TM channel and θ_i is the solar incidence angle. Solar irradiance values were computed by Markham and Barker (Dozier, 1989). Several pairs of calibration coefficients are available. The most used are the pre-launch coefficients provided by EOSAT. From comparison with ground measurements, new calibration coefficients are provided by Gu and others from INRA Montfavet, France. Bourdelles and Fily (1993) use the well-known reflectance of seawater in order to choose the best calibration coefficients. They find that neither EOSAT nor INRA calibration coefficients led to correct values of the seawater reflectance in the infrared channels. Thus, new calibration coefficients were established. To calculate the grain size, the channels TM4, TM5 and TM7 were used successfully.

For each pixel, the apparent reflectance is calculated from the numerical count NC by

$$\rho_{app} = \frac{(a_0 + a_1 NC) \pi}{E_0 \cos(\theta_s - \alpha)}$$

Where θ_s is the solar zenith angle and α the local slope angle. This apparent reflectance is compared with the theoretical modelled reflectances $\rho(r)$ computed for different radii r (Figure 5). The snow grain size r is the radius for which $\rho_{app} = \rho(r)$. In these calculations a single curve was computed for each TM wavelength using the solar azimuth angle as irradiance angle. However, the true irradiance angle is slightly different, due to the local slope. Therefore the curves corresponding to the maximum slope angles appearing on the scene were computed, and for each pixel reflectance, the resulting grain sizes were compared. The maximum error made on grain size using this

approximation is less than 15%. In this investigation the slope angles were estimated using the reflectances from channel TM2.

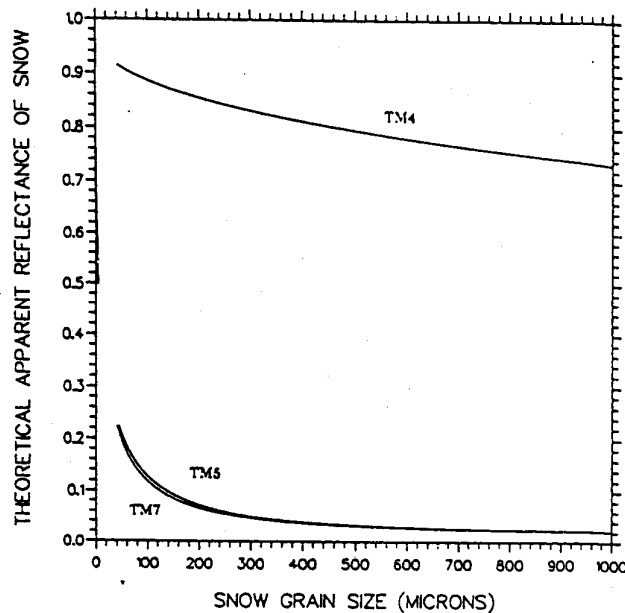


Figure 5 Reflectance of the snow at the top of the atmosphere versus snow grain size, for infrared channels TM4, TM5, and TM7 (Bourdelles, 1993).

According to Wiscombes and Warren's 1980 model results (Wiscombes, 1980), the snow reflectance in channel TM2 is almost independent of grain size and solar incidence angle. An integrated value for the reflectance at the top of the atmosphere was calculated and the assumption was made that the variations over the scene were due to topographic effects. A local slope angle was deduced for each pixel.

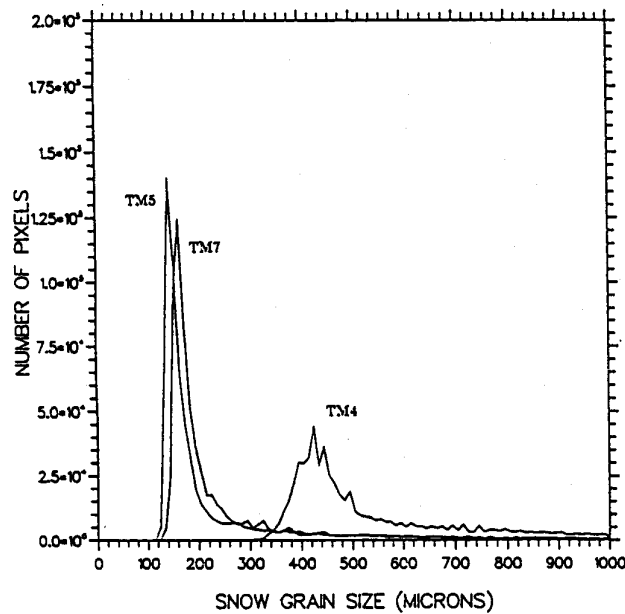


Figure 6 Histograms of snow grain-sizes calculated with TM4, TM5, and TM7 (Bourdelles, 1993).

The results from this investigation showed that the spatial variations of grain sizes are very similar whether obtained from TM4, TM5 or TM7 data. As shown in Figure 6, grain size distribution computed from TM4 is quite different from those obtained from TM5 and TM7. The mean grain size is larger (420-430 μm instead of 145 – 165 μm) and there is more variability.

One reason for the difference between computed radii for TM4, TM5 and TM7 could be the difference in penetration depth. Channels TM5 and TM7 are only sensitive to the surface of the snow cover, while TM4 receives information from the top centimetres, leading to the determination of a greater grain size. At the time of the scene acquisition there was indeed a thin layer of new snow over much older snow.

An alternate explanation would be to suppose that the atmospheric correction model is not sufficiently accurate. By choosing an atmospheric profile with maritime aerosols, snow grain sizes computed with TM4 would have been lowered by about 50 μm .

2.1.1 Ratio between TM channels

Precise slope values are difficult to obtain in mountain areas. Using ratios between channels instead of a single channel minimizes this effect because the slope is independent of the channel. We will use the ratio R_{ij} defined as

$$R_{ij} = \frac{TM_i - TM_j}{TM_i + TM_j} \quad (1)$$

where TM_i is the apparent reflectance or the ground reflectance for channel i .

Dozier (1989) finds some of these ratios to be indices of grain size. In his paper the ratios are between the apparent planetary reflectances. He concludes:

R24 is a grain size index for all sizes. Higher values represent larger grain sizes. It is also sensitive to contamination, but not enough to reliably estimate absorption by impurities.

R25 is also a grain size index and helps to identify larger grains.

R45 is a grain size index for finer grains. Higher values represent larger sizes.

Fily et al. (1997) also have studied the ratios between the TM channels. Figure 7 shows the modelled ratios R_{ij} against grain size for a number of possible combinations, excluding TM1 because this channel is often saturated over snow. Ratios R23, R24, and R34 do not vary much against the grain size. Other computations show that these ratios are not very sensitive to the terrain conditions. R24 is the most important of these because it is most sensitive to grain size and because TM2 is less often saturated than TM3. R25, R26, R35, R37, R45, and R47 are all very similar. They strongly depend on the grain size when the grains are small, but there is a saturation effect for grains larger

than 300 μm . It was found that the ratios including TM5 are more sensitive to the terrain conditions than those including TM7. Among those ratios, R45 and R47 were studied as examples because channel 4 is less sensitive to atmosphere and pollutions than are channels 2 and 3.

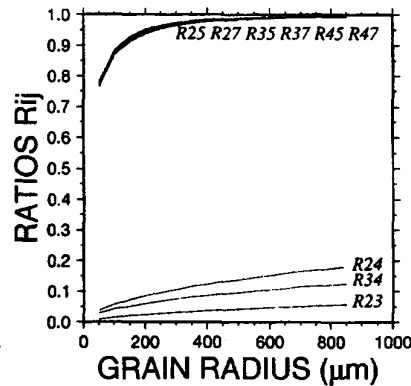


Figure 7 Modelled values of ratios R_{ij} against the grain size. The sun incidence angle is 40° , the view is nadir and the surface is horizontal (Fily, 1997).

Figure 8 gives comparisons between Landsat-derived and computed ratios R24, R45 and R47. The measured data are the surface mean convex radii and the ratios between Landsat-derived reflectances with and without atmospheric corrections. The theoretical ratios are given for a horizontal surface and for six different geometrical conditions: solar incidence angle is 40° and 70° , viewing angle is nadir or 20° , viewing azimuth angle is 0° or 180° in the solar plane.

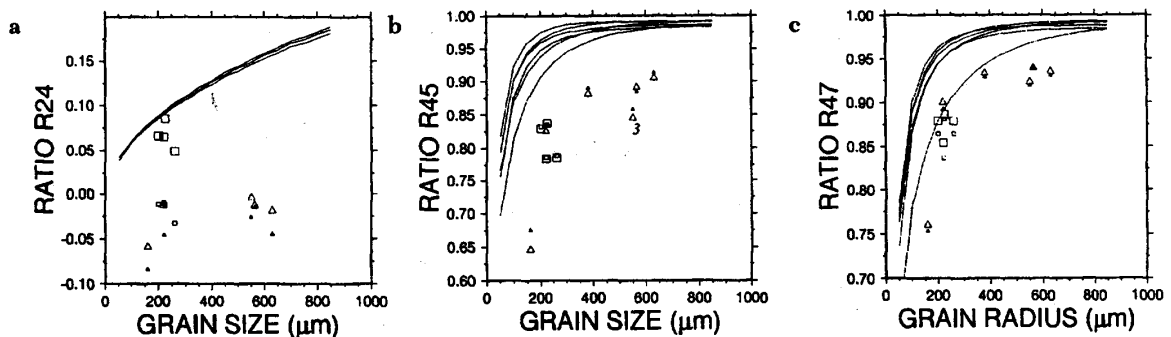


Figure 8 Comparison between modeled and measured ratios R24 (a), R45 (b), and R47 (c). Triangles are for April, squares for December, small symbols are with and large symbols without atmospheric correction. The curves are model results shown for various geometrical conditions. See text. (Fily, 1997).

For R24 all the April measured values are smaller than the theoretical ones. The main reason is snow contamination, which is pretty large in April. The pollution effect is more important for TM2 than TM4, and therefore the measured ratios are a lot smaller. For R45 and R47 the measured data follow the theoretical curves better. The main problem for both cases comes from the saturation of the ratios for large grain size.

Comparing the work of Dozier (1989), one agrees that R24 “is a grain size index for all sizes” if the solar incidence angle is small enough to avoid indirect irradiance effects, but only if the snow is not contaminated and that R45 “is a grain index for finer grains”. But one disagrees that R25 “helps to identify larger grains”, because the behaviour of R25 is similar to that of R45, except for being more dependent on contamination and atmospheric conditions than R45.

In a later work, Fily et al. (1999) tried to use the ratio R45. The behaviour of this ratio matched previous results and theoretical computations well. Yet it was found to be impossible to invert the ratio in order to obtain quantitative results because the slope and the atmosphere effects were not eliminated.

2.2 AVIRIS

Li et al. (2001) have studied grain size retrieval from near-infrared radiances at multiple wavelengths. They used the Airborne Visible/Infrared Imaging Spectrometer (AVIRIS) at wavelengths 0.86, 1.05, 1.24 and 1.73 μm . They adopted a comprehensive radiative transfer model based on the DISORT multiple scattering algorithm (Stamnes, 1988) to account for the bidirectional reflectance of the snow surface. They assumed that the snow grains consist of spherical particles in a single homogeneous layer with a specific grain size.

At 0.86 μm the snow impurities have a non-negligible effect on the reflectance, but only for large grain sizes and large soot concentrations.

AVIRIS is a nadir-viewing instrument with a flight height of 20 km and a ground instantaneous field of view of 20 m. Figure 9 shows the simulated reflectance at satellite level versus snow grain size for AVIRIS channels 54 (0.86 μm), 73 (1.05 μm), 93 (1.24 μm), and 145 (1.73 μm) at a solar zenith angle of 49°. These reflectances were used to estimate the grain size as discussed below.

Satellite-measured radiances I_λ are converted to normalized reflectance R_λ at satellite level for each AVIRIS channel by using $R_\lambda = \pi I_\lambda / S_\lambda \cos \theta_0$, where S_λ is the extraterrestrial solar irradiance and θ_0 is the solar zenith angle. Snow grain size can be retrieved at each channel by comparing measured normalized reflectances R_λ with computed ones. In order to maintain the accuracy of retrieval and save computational time, the computed reflectance (see Figure 9) as a function of grain size are fit with a logarithmic expression of the form:

$$R_\lambda = a_\lambda + b_\lambda \log(r_\lambda) \quad (2)$$

Here R_λ is the computed normalized reflectance and r_λ is the corresponding grain size. The coefficients a_λ and b_λ are obtained by least squares fitting method. Thus, the snow grain size can be retrieved from the satellite-measured radiances using Eq. (2).

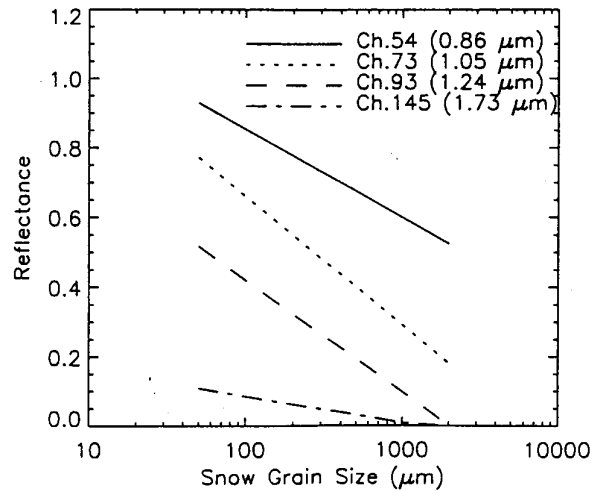


Figure 9 The simulated reflectance (as defined in Eq. (2)) as a function of effective snow grain size at solar zenith angle 49° (Li, 2001).

An AVIRIS image obtained 22:45 GMT on June 4, 1995 over the Arctic Ocean was selected in this study. Figure 10 shows the retrieved snow grain size distribution for this image. The average snow grain size retrieved are 1100, 550, 400 and 60 μm for channels 54, 73, 93, and 145, respectively. This is quite similar to what is shown in Figure 6. The penetration depth increases with decreasing wavelengths, and the snow grain size increases with depth.

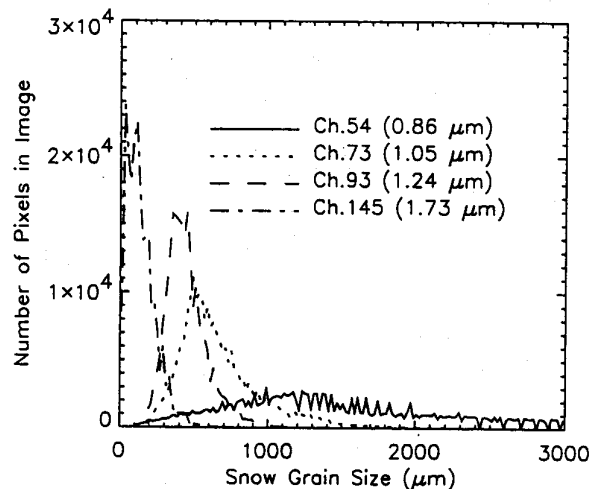


Figure 10 Histogram of retrieved snow grain size from AVIRIS channels 54, 73, 93, and 145 (Li, 2001).

Nolin and Dozier (1993) describes a method for grain size mapping that made use of the spectral capabilities of AVIRIS. Using the DIScrete-Ordinates Radiative Transfer model, DISORT (Stamnes, 1988) they modelled the relationship between snow grain size and a near-infrared reflectance for a wide range of grain radii and solar illumination angles. They showed that, given an atmospherically corrected near-infrared image of

surface reflectance and the illumination and viewing geometries, snow reflectance can be inverted to yield quantitative estimates of snow grain size. They used a single AVIRIS band centred at $1.03\mu\text{m}$ because (a) at that wavelength snow reflectance is highly sensitive to grain size, (b) there is still a strong snow reflectance signal, and (c) the atmospheric transmittance is high. There are two drawbacks to this method; the primary one is the effect of sensor noise when the interpretation is based on the signal in one wavelength band. The second drawback is the requirement for knowledge of the sun and sensor angles.

The same authors (Nolin, 2000) claim to have developed a robust, accurate inversion technique for the grain size in a snowpack's surface layer from imaging spectrometer data. Using a radiative transfer model, the method relates an ice absorption feature, centred at $\lambda = 1.03 \mu\text{m}$, to the optically equivalent grain size. Mainly because of variability in the absorption of ice, the optical properties of snow over the solar spectrum range from nearly complete reflectance to nearly complete absorption. There are several prominent absorption features: one of them extends from $0.96 \mu\text{m}$ to $1.08 \mu\text{m}$ and is centred at $\lambda = 1.03 \mu\text{m}$. In this article the penetration depth is also discussed, and they find that the inversion method derives an optically equivalent grain size for a surface layer whose thickness depends inversely on the snow's density. While snowpack vertical heterogeneity most certainly affects measurements in the shorter wavelengths, use of the $1.03 \mu\text{m}$ absorption feature typically represents just the top 0.5 cm to 3 cm of a snowpack, over which the grain size distribution is more likely to be homogeneous. In the $1.03 \mu\text{m}$ region, vertical heterogeneity would play a role in restricted cases, such as a thin surface crust or where surface hoar has formed.

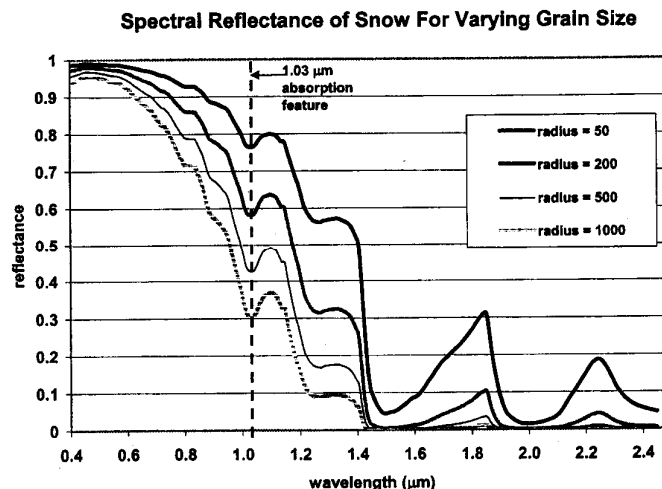


Figure 11 The spectral directional hemispherical reflectance of snow as calculated using the DISORT model (Stamnes, 1988). Each curve represents the spectrum for a different snow grain radius. The dashed line indicates the location of the $1.03 \mu\text{m}$ absorption feature (Nolin, 2000).

The method used in this research is based on an inversion technique developed by Clark and Roush (1984). For ice frosts, they determined the depth of a spectral absorption feature and related it to frost grain size. They recognized that an apparent “continuum” could represent the spectrum in the absence of the absorption feature of interest. Clark and Roush calculated the scaled band depth D_b as the difference between the

continuum reflectance R_c and the reflectance spectrum R_b in the deepest part of the absorption band, normalized by the continuum reflectance:

$$D_b = \frac{R_c - R_b}{R_c}$$

Figure 12 shows the snow spectral reflectance and continuum reflectance for the absorption features centred at $1.03 \mu\text{m}$, derived from AVIRIS measurements. The advantage of scaling the band depth by the continuum reflectance is that the grain size estimates become independent of the absolute magnitude of the reflected radiance, and thereby are not sensitive to topography. The solar illumination angle changes the magnitude of the reflectance spectrum, but changes neither the shape nor relative depth of the absorption feature.

While this band-depth method is a valuable approach to the problem, its reliance on a single spectral band causes the accuracy of the results to suffer in the presence of noise in the reflectance spectrum. Noise-induced changes in the spectrum affect the depth of the absorption feature and may give erroneous grain size estimates.

To minimize any effects of noise on grain size retrievals, this investigation used the scaled area of the absorption feature, A_b , rather than the simply scaled band depth.

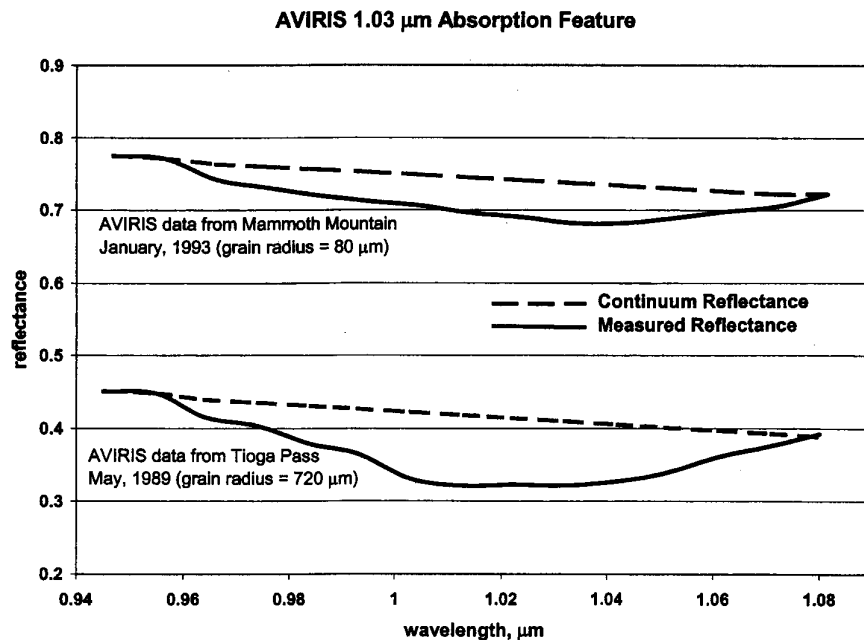


Figure 12 The $1.03 \mu\text{m}$ absorption feature from two AVIRIS snow reflectance spectra from Mammoth Mountain in 1993 and Tioga Pass in 1989. The continuum reflectance is plotted as the dashed line across the top of each feature. Derived grain sizes are shown for each location (Nolin, 2000).

Scaled band area is a dimensionless quantity and is calculated by integrating the scaled absorption band depth over the wavelengths of the absorption feature:

$$A_b = \int_{\lambda} \frac{R_c - R_b}{R_c}$$

The basic assumption is that the noise is randomly distributed Gaussian noise. While the exact distribution of sensor noise is not known, a normal distribution is a reasonable assumption. By integrating over the absorption feature, the fluctuations caused by noise should average out and produce an estimate closer to the true value.

The “scaled band-area” mapping technique requires that radiometrically calibrated imaging spectrometer data be atmospherically corrected to obtain surface reflectance. The data do not need to be corrected for topographic and anisotropic scattering effects. To accurately map the absorption feature, the end points of the feature must be located. Since noise may be present in the measured reflectance spectrum, the continuum end points are established by averaging the reflectance values for pairs of AVIRIS bands centred at $\lambda = 0.95 \mu\text{m}$, $0.96 \mu\text{m}$ and at $\lambda = 1.08 \mu\text{m}$, $1.09 \mu\text{m}$. The continuum-scaled band depth for each channel is calculated and integrated using the trapezoidal rule to determine the scaled area of the absorption feature. In this investigation 17 AVIRIS channels were used. It is worth noting that for the AVIRIS data used in this study, the source of spectral noise appears to be solely from the sensor, rather from the atmospheric correction method. There is virtually no difference in the shape of the absorption feature before and after atmospheric correction, because this absorption feature is located in a spectral region where atmospheric scattering and absorption are small, especially in the dry, high visibility conditions under which the AVIRIS data were acquired.

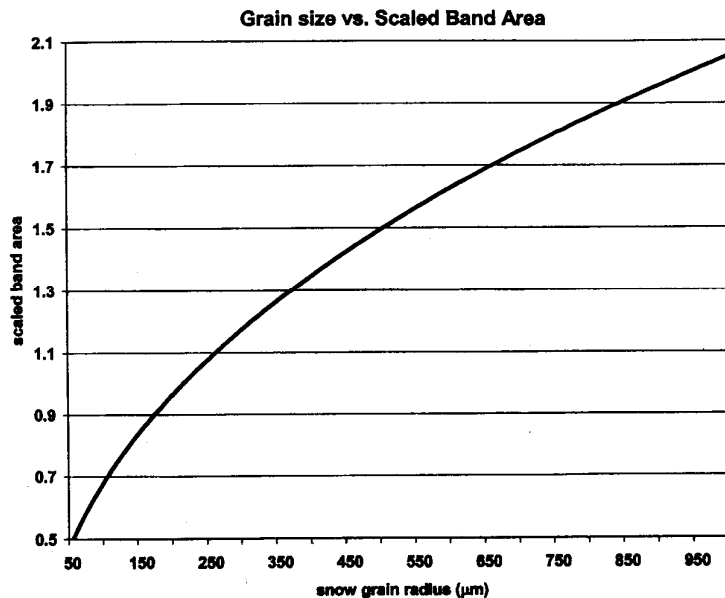


Figure 13 The nonlinear relationship between snow grain radius and scaled band area. Scaled dimensionless band areas were computed with DISORT (Nolin, 2000).

In parallel, the DISORT model was used to calculate spectral reflectance for the same 17 AVIRIS channels for a wide range of snow grain radii. For each grain size a scaled

band area was calculated from the model derived spectrum and a lookup table was created, in which the scaled band areas are juxtaposed with their corresponding snow grain radii.

AVIRIS images from Mammoth Mountain, Sierra Nevada, January 11, 1993 and Tioga Pass, Sierra Nevada, May 26, 1989 were used together with ground based snow spectral reflectance data collected with an Analytical Spectral Devices Full-Range (ASD-FR) field spectrometer in three locations: a site on the western portion of Greenland ice sheet; Lake Mendota, Wisconsin; and Pumice Valley, California. Figure 14 shows that scaled band area estimates of snow grain size were very similar to those measured from snow samples with no apparent bias.

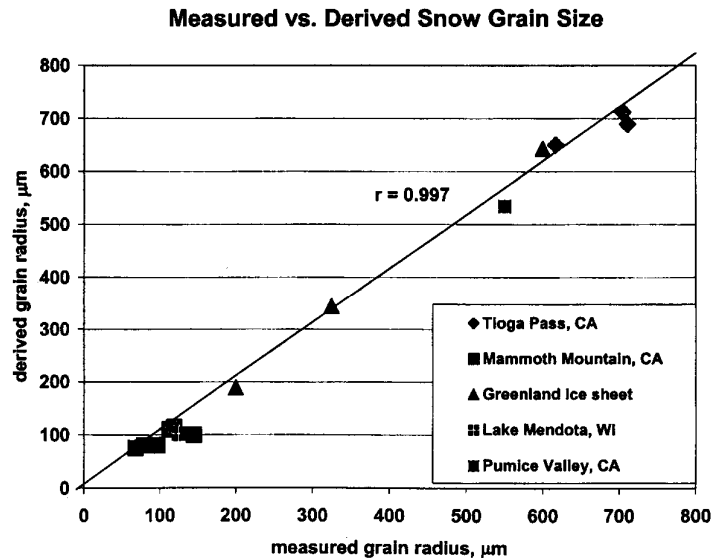


Figure 14 Scatterplot showing the correlation between measured snow grain size and grain size derived from both airborne (AVIRIS) and ground-based (ASD-FR) spectrometer measurements (Nolin, 2000).

2.3 SAR

Shi and Dozier (2000) describe a work on estimation of snow parameters using SIR-C/X-SAR. Snow depth and optical equivalent grain size were estimated from a physically-based first order backscattering model through analysis of the importance of each scattering term and its sensitivity to snow properties. The relationship between the simulated scattering coefficients and the optically equivalent particle size can be written as

$$r_s = \left(\frac{0.01\kappa_s(X)}{2V_s S_f (2.8332 + 6.6143V_s)} \right)^{1/3}$$

Where r_s is in cm. V_s is the volume fraction of ice, S_f is the structure factor for a single particle system

$$S_f = \frac{(1 - V_s)^4}{(1 + 2V_s)^2}$$

The scattering coefficient $\kappa_s(X)$ can be obtained from the estimated $\kappa_s(X)$ and the albedo $\omega(X)$ at each pixel. The algorithm is based on the assumption of a single dry snow layer over a rock or soil surface.

A number of snow pits were dug and snow particles were measured (more than 200 grains in each pit). Figure 15 (A) shows the ice particle distribution from one snow pit. The snow pack has a large size variation. In order to verify the algorithm, the grain size measurements from each snow pit were processed to an “optically equivalent” particle radius to represent the “ground truth”. Figure 15 (B) compares the snow particle radius between the ground measurements and those estimated from the SIR-C/X-SAR image data.

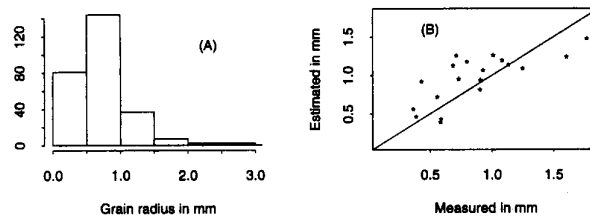


Figure 15 (A) Histogram of the particle radius distribution measured in a snow pit. (B) Comparison of the optically equivalent particle radius from the field measurement with that estimated from Sir-C/X-SAR image data (Shi, 2000).

Validation using three SIR-C/X-SAR measurements from C-band VV, HH, and X-band VV, showed that the algorithm performs usefully for incidence angles greater than 30° with RMSE of 0.27 mm for estimating ice optical equivalent particle radius.

The advantage of this algorithm is that it is physically based and is developed under a pure remote sensing concept. It requires no ancillary data, except for a DEM for calculation of incidence angle at the air-snow interface and fir terrain calibration of SAR measurements. One problem is that C-band SAR measurements are affected mainly by the soil properties. The snow-ground interface interaction terms account for a significant amount of backscattering signal from a snowpack. The algorithm was developed under the assumption that the snow-covered ground is either soil or rock. It is not applicable for the conditions where the signal under the snow cover is generated by volume scattering, such as firn on a glacier.

3 Conclusions

One purpose of the study was to select a method that could be used for estimation of grain size in MODIS images. As the Landsat satellites have spectral bands that are close to bands in the MODIS sensor, it was natural to look at the methods developed for Landsat. The problem of the influence of slopes on the reflected light is minimized by

using ratios between two channels as an index for grain size. A number of ratios of the form

$$R_{ij} = \frac{TM_i - TM_j}{TM_i + TM_j}$$

have been tested. We have selected the R47 as the best. By Fily et al. (1997) it is reported that the measured data matches the theoretical curves well. From the figures it seems that it is even better than R45. The main problem comes from saturation of the ratio for large grain sizes. The ratio is a simple method. You only have to use the signals in two channels and do not need information about the terrain as you need in other methods. The studies do not give a calibrated ratio. One specific ratio value does not give an exact grain size value. It is also a problem how to define the grain size. But the ratio can be used as an index of grain size, the ratio increases with increasing grain size up to the point of saturation.

The wavelengths of the Landsat ETM+ bands are

Band 4: 0.775 – 0.900 μm

Band 7: 2.09 – 2.35 μm

The MODIS bands closest to these are

Band 2: 0.841 – 876 μm

Band 7: 2.105 – 2.155 μm

Band 2 has a spatial resolution of 250 m and band 7 has 500 m. This means that the grain size index R27 can be found with 500 m resolution.

Studies of calculated grain size from the R27 ratio, show that the index is well suited for monitoring the changes in grain size due to precipitation and temperature changes. The index increases with increasing temperature and gets a lower value when new snow has fallen. To make a prediction of the wetness in the snow, one can use a combination of snow temperature and grain size index. If the grain size increases rapidly near 0 °C, it is a sign of wet snow. Melting and freezing make the grains grow fast.

The grain size index for snow for MODIS images, lies between approximately 0.7 and 1.0. Bare ground of different kinds has low index values. 0.7 is not an exact threshold value for snow. Somewhere around 0.7 the index shows that there is probably some snow on the ground. To be sure that the index shows snow grain size, one should use a snow classification algorithm in addition to check if there really is snow on the ground.

4 References

- Bronge, L. B. Bronge C. 1999. Ice and Snow-Type Classification in the Vestfold Hills, East Antarctica, Using Landsat-TM Data and Ground Radiometer Measurements. *International Journal of Remote Sensing*, Vol. 20, No. 2, p. 225-240.
- Bourdelles, B. Fily, M. 1993. Snow Grain-Size Determination from Landsat Imagery over Terre Adélie, Antarctica, *Annals of Glaciology*, Vol. 17, p. 86-92.

- Clark, R. N., and Roush, T. (1984), Reflectance spectroscopy: Quantitative analysis techniques for remote sensing applications. *J. Geophys. Res.* 89: 6329-6340
- Dozier, J. Schneider, S. R., McGinnis, D. F. 1981. Effect of Grain Size and Snowpack Water Equivalence on Visible and Near-Infrared Satellite Observations of Snow. *Water Resources Research*, Vol. 17, p. 1213-1221.
- Dozier, J. Marks, D. 1987. Snow Mapping and Classification from Landsat TM Data. *Annals of Glaciology*, Vol. 9, p. 97-103.
- Dozier, J., 1989 Spectral signature of Alpine snow cover from the Landsat Thematic Mapper. *Remote Sensing of Environment*, Vol. 28, p. 9-22.
- Dozier, J. 1989. Estimation of Properties of Alpine Snow from Landsat Thematic Mapper. *Advanced Space Research*. Vol. 9. No. 1, p. 207-215.
- Fily, M. Bourdelles, B. Dedieu, J.P. Sergent, C. 1997. Comparison of In Situ and Landsat Thematic Mapper Derived Snow Grain Characteristics in the Alps. *Remote Sensing of Environment*, Vol. 59, No. 3, p. 452-460.
- Fily, M. Dedieu, J. P., Durand, Y. 1999. Comparison between the Results of a Snow Metamorphism Model and Remote Sensing Derived Snow Parameters in the Alps. *Remote Sensing of Environment*, Vol. 68, p. 254-263.
- Kelly, R. E. J., Chang A. T. C., Tsang, L., Chen, C. T. 2002. Parameterization of snowpack grain size for global satellite microwave estimates of snow depth. *IGARSS 2002*.
- Li, W., Stamnes, K., Chen, B. 2001. Snow grain size retrieved from near-infrared radiances at multiple wavelengths. *Geophysical Research Letters*, Vol.28, No. 9, p. 1699 –1702.
- Macelloni, G., Paloscia S., Pampaloni, P., Ruisi, R., Tedesco, M. 2002. Microwave emission of snow in Alpine regions and the detection of surface hoar. *IGARSS 2002*.
- Nolin, A. W., Dozier, J. 1993. Estimating Snow Grain Size Using AVIRIS Data. *Remote Sensing of the Environment*, Vol. 44, p. 231-238.
- Nolin, A. W., Dozier, J. 2000. A Hyperspectral Method for Remotely Sensing the Grain Size of Snow. *Remote Sensing of Environment*, Vol. 74, p. 207-216.
- Orheim, O., Lucchitta B. K. 1987. Snow and Ice Studies by Thematic Mapper and Multispectral Scanner Images. *Annals of Glaciology*, Vol. 9, p. 109-118.
- Orheim, O., Lucchitta, B. K. 1988. Numerical Analysis of Landsat Thematic Mapper Images of Antarctica: Surface Temperatures and physical properties. *Annals of Glaciology*, Vol. 11, p. 109-119.
- Pattyn, F., Declair, H. 1993. Satellite Monitoring of Ice and Snow Conditions in the Sør Rondane Mountains, Antarctica. *Annals of Glaciology*, Vol. 17, p. 41-48.
- Shi, J., Dozier, J. 2000. Estimation of Snow Water Equivalence Using SIR-C/X-SAR, Part II: Inferring Snow Depth and Particle Size. *IEEE Transactions on Geoscience and Remote Sensing*, Vol. 38, No. 6, p. 2475-2488.
- Stamnes, K., Tsay, S., Wiscombe, W., and Jayaweera, K. 1988. Numerically stable algorithm for discrete-ordinate-method radiative transfer in multiple scattering and emitting layered media. *Appl. Opt.* 27, p. 2502-2509.

Winther, J. G. 1993. Studies of Snow Surface Characteristics by Landsat TM in Dronning Maud Land, Antarctica. *Annals of Glaciology*, Vol. 17, p. 27-34.

Winther, J.-G. 1993. Snow and glacier ice characteristics measured using Landsat TM data, Doktor Ingeniøravhandling, Institutt for vassbygging, Trondheim, IVB-rapport B-2-1993-5, ISBN 82-7119-552-2.

Wiscombe, W. J., Warren, S. G. 1980. A model for the spectral albedo of snow. I. Pure snow. *Journal of the Atmospheric Sciences*, Vol. 37 (12), p. 2712-2733.